Fish and Shellfish Immunology 93 (2019) 144–152

Contents lists available at ScienceDirect

Fish and Shellfish Immunology

journal homepage: www.elsevier.com/locate/fsi

Full length article

Characterization and role of PGK from *Litopenaeus vannamei* in WSSV infection

Fei-Xiang Li, Yong-Sheng Zhang, Cui-Luan Yao*

Fisheries College, Jimei University, Xiamen, 361021, PR China

ARTICLE INFO

Keywords:
Litopenaeus vannamei
PGK
RNAi
WSSV
Metabolism
Immune response

ABSTRACT

Phosphoglycerate kinase (EC 2.7.2.3, PGK) catalyses the reversible transfer of a phosphate group from 1,3-diphosphoglyceric acid and ADP to produce 3-phosphoglyceric acid and ATP, which represents the initial production of ATP during glycolysis; therefore, PGK is a key enzyme in the energy metabolism. To study the role of PGK in the resistance to WSSV infection in shrimp, the full-length cDNA of the PGK gene (*LvPGK*) from *Litopenaeus vannamei* was obtained by using homology cloning and RACE amplification. The tissue distribution of *LvPGK* and its expression changes in the main immune tissues after WSSV stimulation were obtained by quantitative real-time PCR. Furthermore, RNA interference (RNAi) was used to study the role of *LvPGK* in shrimp defending against WSSV infection. The results showed that the full-length cDNA sequence of *LvPGK* was 1855 bp, contained a 1248 bp open reading frame (ORF) encoding 415 amino acids, and included a conserved PGK domain. *LvPGK* presented ubiquitous expression in most examined tissues, with the most predominant expression in the muscle and the weakest expression in the intestine. *LvPGK* transcripts could be induced in the hemocytes and hepatopancreas by injection with WSSV. Both the replication of WSSV and the shrimp cumulative mortality decreased significantly after *LvPGK* knockdown ($P < 0.01$). After challenging *LvPGK* RNAi shrimp with WSSV, the concentration of glucose in the hepatopancreas and muscle tissue did not show significant change; however, the content of pyruvate and lactate decreased significantly ($P < 0.05$). Moreover, significant decreases in the expression levels of crustin, ALF1, ALF2 and ALF3 were also detected. The results suggested that *LvPGK* might be involved in WSSV replication by increasing host aerobic and anaerobic metabolism.

1. Introduction

Shrimp culture has suffered from a global disease crisis that has caused considerable economic losses to the aquaculture industry in the past thirty years [1]. Reports have indicated that approximately 60% of shrimp diseases are caused by viruses [2]. Among which, white spot syndrome virus (WSSV) is one of the most prevalent, widespread and lethal for shrimp populations [3].

Lacking an acquired immune system, shrimp mainly rely on their innate immune system to response the pathogenic infection, which might collaborate with many physiological processes. Previous investigations demonstrated that energy metabolism might be involved in the disease-resistance immune response of shrimp [4]. For example, Li and colleagues indicated viral infections could trigger metabolic changes in host cells to support the high bioenergetic and biosynthetic demands of viral replication [5]. In addition, some energy metabolic enzymes might play an important role in shrimp defending against WSSV infection [6–9].

$$1,3-\text{disphosphoglyceric acid} + \text{ADP} \overset{\text{PGK}}{\leftrightarrow} 3-\text{phosphoglyceric acid} + \text{ATP}$$

Previous studies indicated that the mutation of mammalian PGK might lead to chronic haemolytic anaemia [11] and PGK could be involved in the development of a variety of tumours [12–14]. In addition, PGK might contribute to mRNA synthesis of Sendai virus at the elongation step *in vitro* [15]. Therefore, PGK has become a candidate molecule in the development of anti-infection vaccines and drugs in recent years [16,17].

During glycolysis, glucose is phosphorylated, converted, cleaved and yields 1,3-diphosphoglycerate, which is catalysed by PGK to produce 3-phosphoglycerate and then converted into pyruvate. Pyruvate enters into the tricarboxylic acid cycle (TCA) or generates lactate depending on aerobic and anaerobic conditions [18]. Previous studies demonstrated that increased glucose and lactate contents were detected in the hepatopancreas after shrimp *Litopenaeus vannamei* infected with hypodermal and haematopoietic necrosis virus (IHHNV), suggesting

* Corresponding author.
E-mail address: clyao@jmu.edu.cn (C.-L. Yao).

https://doi.org/10.1016/j.fsi.2019.07.048
Received 15 April 2019; Received in revised form 12 July 2019; Accepted 17 July 2019
Available online 18 July 2019

Table 1
PCR primers used in this study.

Primer name	Primer sequences (5′-3′)	Usage
PGK-F	GACGGAGCAAGCAGACAT	Amplification of homologous fragment
PGK-R	GTCCCTAAGAAATGGAAGTG	
PGK-3′-F1	CCCTGTGGTGTGTTTGAAT	First round for 3′RACE
PGK-3′-F2	GTGGCAGCACTCACAGATG	Second round for 3′RACE
PGK-5′-R1	CATTCACATACACATCTCCAAG	First round for 5′RACE
PGK-5′-R2	GGTGAGAGCAAAGGACGACA	Second round for 5′RACE
dsPGK-T7-F1	**GGATCCTAATACGACTCACTATAGG**TGAGGAAACTTGGAGATGTGTATGT	Synthesis of ds*Lv*PGK
dsPGK-R1	TCTACTACCATATCCATGACAGCCT	
dsPGK-F2	TGAGGAAACTTGGAGATGTGTATGT	
dsPGK-T7-R2	**GGATCCTAATACGACTCACTATAGG**TCTACTACCATATCCATGACAGCCT	
dseGFP-T7-F1	**GGATCCTAATACGACTCACTATAGG**ACAAGTTCAGCGTGTCCG	Synthesis of dseGFP
dseGFP-R1	TCGCCGATGGGGGTGTTC	
dseGFP-F2	ACAAGTTCAGCGTGTCCG	
dseGFP-T7-R2	**GGATCCTAATACGACTCACTATAGG**TCGCCGATGGGGGTGTTC	
qVP28-F	ATCCGCAATGGAAAGTCTGA	Absolute qPCR
qVP28-R	GGGTGAAGGAGGAGGTGTT	
qPGK-F	ACAAATTGATCGCAAAGGC	Immune gene expression analysis
qPGK-R	TGGTCCACAGTCCAGTCCC	
qβ-actin-F	GAAGTAGCCGCCCTGGTTGT	
qβ-actin-R	GGATACCTCGCTTGCTCTGG	
qCrustin-F	GGAGGGTCAAGCCTACTGC	
qCrustin-R	ACGTGGGCATGTGGGAC	
qALF1-F	GGATGTGGTGTCCTGGATGG	
qALF1-R	GCGTCGTCCTCCGTGATG	
qALF2-F	GCGAACAAACTCACTGGACTG	
qALF2-R	ACATGCGACCCTGGAATACAG	
qALF3-F	GACCTGTCCAACCCTGAGC	
qALF3-R	TCGCCTCCTCCTCCGTTATC	

Note: The bolded letter represents the T7 RNA polymerase promoter sequence.

Table 2
Predicted PGK protein sequences used for multiple sequence alignments and phylogenetic analysis.

Species	GenBank Acc. NO.	Protein	Identity (%)
Homo sapiens	NP_000282.1	PGK	75.1
Mus musculus	AAA70267.1	PGK	74.3
Danio rerio	NP_998552.1	PGK	72.9
Oryzias latipes	XP_004076818.1	PGK	72.4
Drosophila melanogaster	ABH06602.1	PGK	74.9
Tribolium castaneum	XP_968140.1	PGK	73.6
Danaus plexippus	EHJ66818.1	PGK	79.5
Pararge aegeria	JAA78662.1	PGK	78.6
Spodoptera frugiperda	ALA09393.1	PGK	80.0
Hyalella azteca	XP_018025899.1	PGK	81.5

that the virus might achieve replication and proliferation by changing the host's metabolic pathways [19].

Antimicrobial peptides (AMPs) play a major role in the innate immunity of shrimp against microbial invasion by directly killing foreign pathogens. Crustin and anti-lipopolysaccharide factor (ALF) are the crucial members of AMPs [20,21] and exhibit potential antimicrobial-activity against a broad range of pathogens, including WSSV [22–24]. However, till to the present study, the molecular and expression characterizations of PGK in crustacean have not been reported, and the role of PGK in shrimp response to WSSV infection is poorly understood.

In the present study, the full-length cDNA sequence of PGK was first cloned from *L. vannamei*, and the temporal expression profiles of the *LvPGK* after WSSV challenge were investigated. Furthermore, the role of PGK in shrimp response to WSSV infection was studied by using RNA interference (RNAi) approach, in order to better understanding the potential role of PGK in shrimp immune response.

2. Materials and methods

2.1. Animals, WSSV challenge and sample collection

L. vannamei (8.44 ± 1.35 g weight) were purchased from a commercial shrimp farm in Xiamen, China. Before experiment, shrimp were acclimated for 7 days at 28 °C at a salinity of 25 practical salinity units (psu) in recirculating seawater tanks and fed with commercial diets every day. The tissues including gill, heart, stomach, brain, hepatopancreas, nerve, intestine, muscle and hemocytes were dissected out or collected from 3 healthy shrimps as our previous report [25]. All samples were preserved in liquid nitrogen for RNA extraction.

Shrimp immune challenge was carried out by intramuscularly injection of 50 μl WSSV (5×10^7 copies) in phosphate buffered saline (PBS, 137 mM NaCl, 2.7 mM KCl, 1.8 mM KH_2PO_4, 10 mM Na_2HPO_4) into the second abdominal segment. Shrimp were injected with 50 μl PBS as the control. The hepatopancreas and hemocytes of each group were collected at 6, 12, 24, 48 and 96 h after WSSV injection. The hemocytes and hepatopancreas pooled from 3 shrimps at each time point were mixed as one sample; and every treatment was composed of three replicates (N = 3). All samples were frozen in liquid nitrogen immediately and then transferred to a −80 °C freezer for further experiments.

2.2. Total RNA extraction and cDNA synthesis

Total RNA was extracted using the Eastep® Super Total RNA Extraction Kit (Promega, USA) according to the manufacturer's instructions. First strand cDNA was synthesized using the GoScript™ Reverse Transcription System Kit (Promega, USA) with 1 μg of total RNA. The cDNA products were used for the *LvPGK* gene amplification as well as quantitative real-time PCR (qPCR) and double-stranded RNA (dsRNA) synthesis.

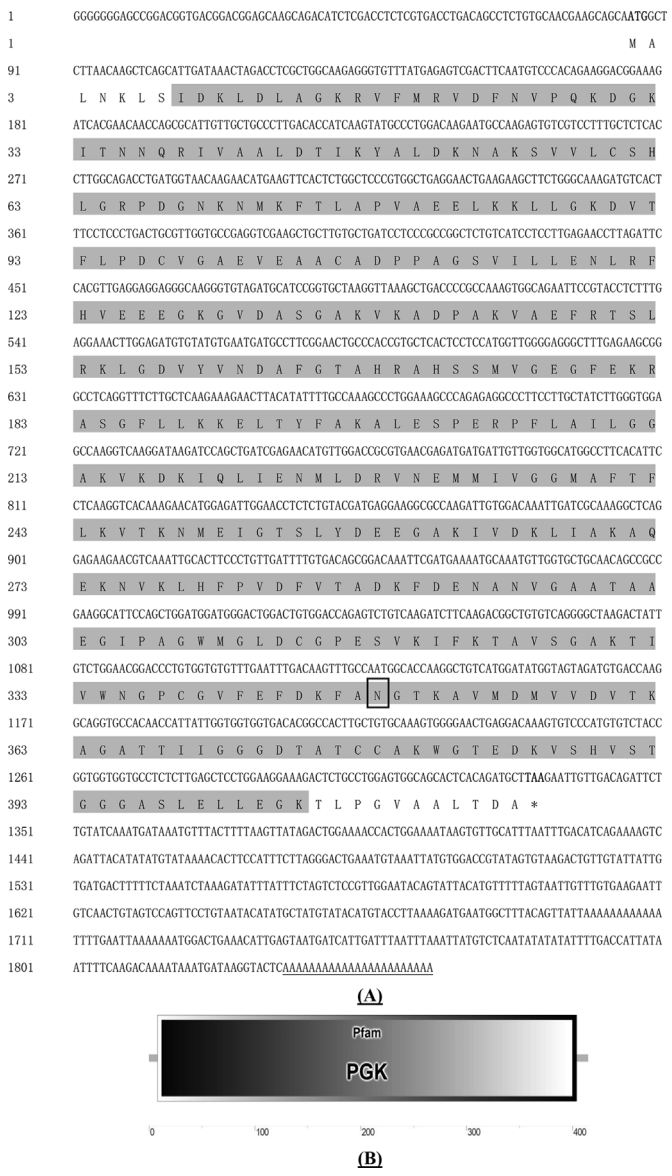

Fig. 1. Sequence analysis and predicted domain of *Lv*PGK. (A) Full-length cDNA sequence and deduced amino acid sequence of *Lv*PGK. The bolded letter indicates the start codon and stop codon, respectively. The boxed information indicates the predicted N-glycosylation site. The shading indicates the predicted PGK domain. The underline indicates the predicted polyA signal. (B) Deduced PGK domain of *Lv*PGK was predicted by SMART.

2.3. LvPGK cDNA cloning and sequence analysis

The PGK cDNA fragment was amplified using primers PGK-F and PGK-R with muscle cDNA as the template at an annealing temperature of 53 °C. The 3′ end PCR amplification of the *LvPGK* was performed using the gene-specific primers PGK-3′ F1/PGK-3′ F2 and the adaptor primers AOLP/AP with nested PCR and annealing temperatures of 53 °C and 56 °C, respectively. For the 5′ end, template was prepared using muscle tissue as our previous report [25], and the nested PCR was performed with primer pairs AAP/PGK-5′ R1 and AP/PGK-5' R2 at an annealing temperatures of 53 °C and 59 °C, respectively. The primer sequences are shown in Table 1. All PCR products were gel-purified, ligated, cloned and sequenced as our previous report [26].

The deduced amino acid sequence was analysed with the Expert Protein Analysis System (EXPASY) (http://www.expasy.org). The protein domain feature and the glycosylation site were predicted by Simple Modular Architecture Reach Tool (SMART) (http://smart.embl-heidelberg.de) and NetNGlyc 1.0 Server (http://www.cbs.dtu.dk/services/NetNGlyc/), respectively. The predicted PGK proteins from different species (Table 2) were assessed via multiple sequence alignment using the Clustal Omega (http://www.ebi.ac.uk/tools/msa/clustalo/), and then a phylogenetic tree was constructed using the neighbour-joining (NJ) method in MEGA 5.0 software. Bootstrap sampling was reiterated 1000 times.

2.4. Tissue distribution and expression analysis after WSSV challenge

The tissue expression and transcriptional levels of *LvPGK* in the hemocytes and hepatopancreas of WSSV-infected shrimp were investigated using qPCR with the specific primers qPGK-F/qPGK-R and the GoTaq® qPCR Master Mix Kit following the manufacturer's instructions. The internal reference gene *Lvβ-actin* in shrimp was used with the primers qβ-actin-F/qβ-actin-R (Table 1). The reaction process included the following steps: denaturation at 94 °C for 2 min, 40 cycles of 94 °C for 15 s, and annealing temperature of 60 °C for 1 min. The expression of the target gene was calculated with the $2^{-\triangle\triangle CT}$ method [27].

2.5. Synthesis of dsRNA

Double-stranded RNA (dsRNA) was synthesized *in vitro* according to the method of Wang and colleagues [28]. The primers dsPGK-T7-F1/dsPGK-R1 and dsPGK-F2/dsPGK-T7-R2 were designed according to the ORF of our obtained *LvPGK* cDNA sequence. The domain fragment of the *LvPGK* gene containing the T7 RNA polymerase promoter sequence was amplified by PCR. The products were taken as a sense chain and antisense chain respectively, and ds*LvPGK* with a length of 622 bp was synthesized according to the instructions of the T7 RiboMAX™ Express RNAi System (Promega, USA). Similarly, the primer pairs dseGFP-T7-F1/dseGFP-R1 and dseGFP-F2/dseGFP-T7-R2 were designed according to the enhanced green fluorescent protein (eGFP) vector to synthesize dseGFP with a length of 500 bp as the control.

2.6. RNA interference of LvPGK assay

Healthy *L. vannamei* (1.83 ± 0.65 g weight) were acclimated for at least 7 days as described above. RNAi was performed by injecting 20 μl ds*LvPGK* (3 μg/g shrimp) into the second abdominal segment of each shrimp. Shrimp were injected with 20 μl of dseGFP as the control. The interference effect of ds*LvPGK* was confirmed by detecting the expression of *LvPGK* using qPCR with muscle cDNA (N = 3) at 24 h and 48 h after dsRNA injection.

2.7. WSSV copy numbers and cumulative mortality of shrimp

To investigate the impact of *LvPGK* knockdown on WSSV replication and shrimp mortality, the shrimp were injected intramuscularly with 3 μg/g ds*LvPGK* dissolved in PBS. The shrimp were injected with same amount PBS or dseGFP as control. After 24 h ds*LvPGK* injection, the shrimp were injected with 20 μl WSSV (2×10^7 copies). The muscle pooled from 3 shrimps at each time point were mixed as one sample, and three parallel samples were collected at 24 h and 48 h (N = 3). Genomic DNA was extracted from shrimp muscle by a commercial kit (Tiangen, China), and the WSSV copy numbers in each sample were detected by absolute qPCR with primers qVP28-F/qVP28-R according to the method of Qiu et al. [29]. Shrimp cumulative mortality was evaluated by calculating the numbers of dead animals (shrimp injected with PBS or dseGFP as control) every 12 h after WSSV injection within 48 h.

2.8. Biochemical assay and gene expression analysis

To investigate the effect of *LvPGK* silencing on the metabolism

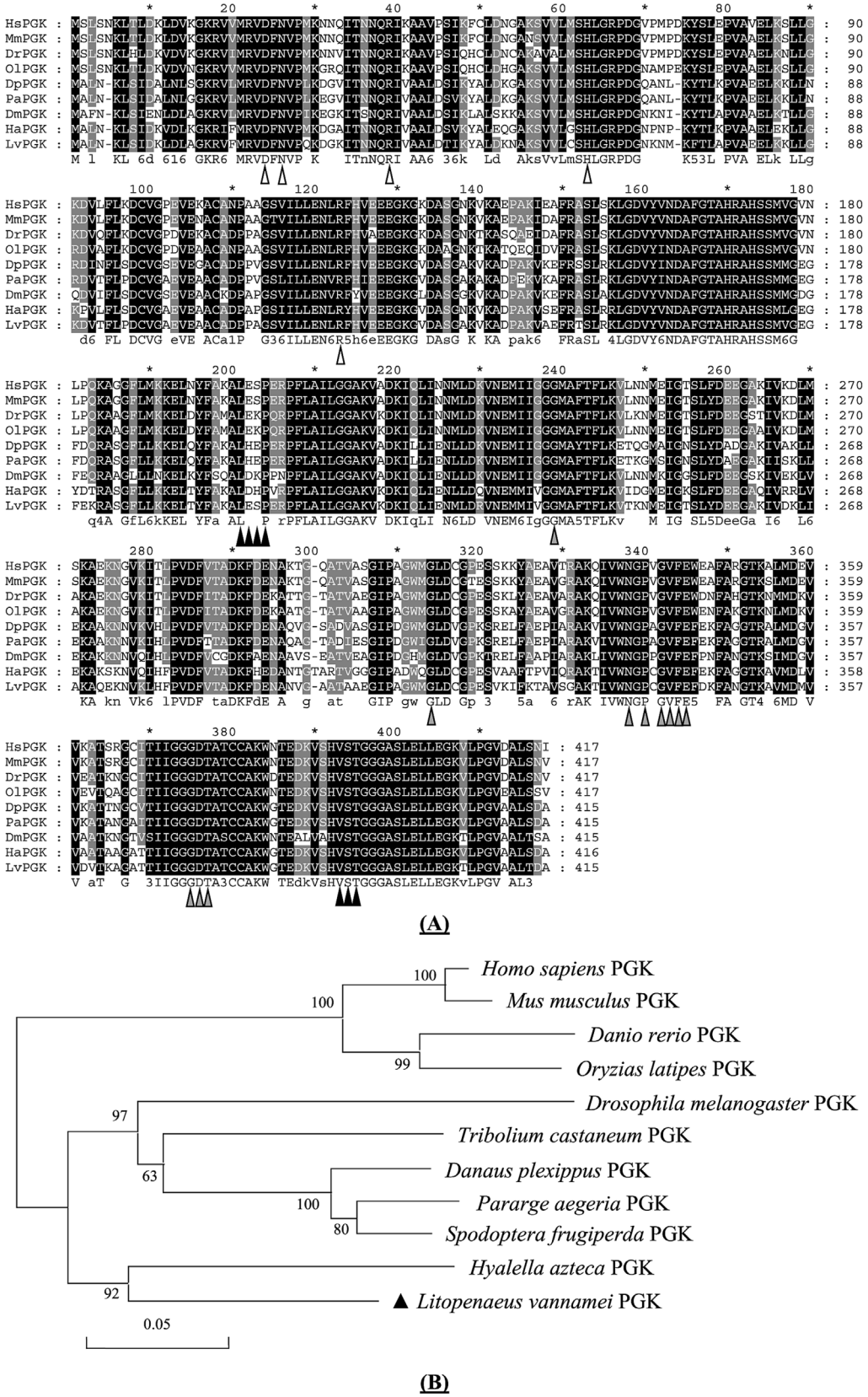

Fig. 2. Conservative domain and phylogenetic analysis of the PGK. (A) Multiple sequence alignments of PGK amino acids from different species. The predicted substrate binding sites, ADP binding sites and hinge region were white triangles, grey triangles and black triangles, respectively. (B) Phylogenetic tree (NJ) based on the predicted PGK amino acid sequences. The scale bar corresponds to 0.05 estimated amino acid substitutions per site. The bootstrap value was tested 1000 times (bootstrap = 1000). The *Lv*PGK protein was marked with a black triangle. The GenBank accession numbers of these deduced PGK are listed in Table 2.

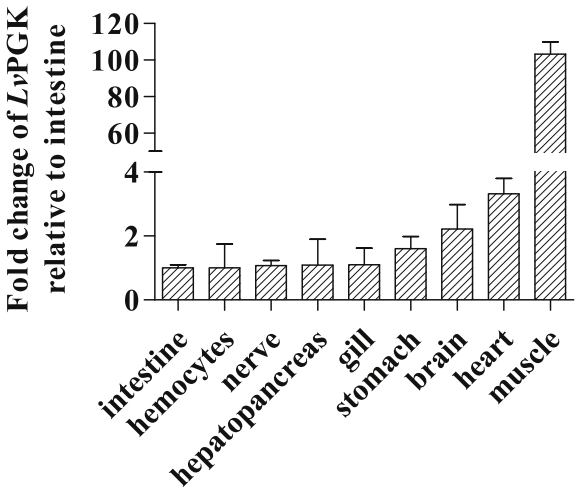

Fig. 3. Tissue expression profiles of *Lv*PGK. The relative expression levels of *Lv*PGK in different tissues were compared against that in intestine. Bars indicate the mean ± SE of three independent cDNA samples (N = 3).

during shrimp defending against WSSV infection, the concentration of glucose, pyruvate and lactate were detected in *LvPGK* silencing shrimp after WSSV injection. WSSV challenge in *LvPGK* silencing shrimp was carried out as above. The hepatopancreas and muscle were dissected and collected at 0 h, 24 h and 48 h after WSSV injection. The tissues pooled from 3 shrimps at each time point were mixed as one sample, and each sample had triplicates (N = 3), and the tissues were homogenized with PBS (10% W/V) and then centrifugated at 4 °C. The supernatants were used for further biochemical detection. All biochemical assays were performed using detection kits according to the manufacturer's instructions (Jiancheng, Nanjing). The total protein concentration assay was performed with the BCA method [30].

To research the role of *LvPGK* in shrimp defending against WSSV infection, the expression of some immune genes including crustin, ALF1, ALF2 and ALF3 were examined in *LvPGK* silencing shrimp after WSSV injection. Total RNA was extracted from hepatopancreas of *LvPGK* or eGFP silencing shrimp at 0 h, 24 h and 48 h after WSSV infection. The cDNA synthesized and expression levels of crustin, ALF1, ALF2 and ALF3 were determined as above. The gene specific primers were used for the qPCR amplifications and *Lvβ-actin* as internal reference (Table 1). All data were given in terms of mRNA relative expression as mean ± SE (N = 3).

2.9. Statistical analysis

The data were analysed by an independent sample *t*-test using SPSS 19.0 software for Windows, and differences were considered a significant at $P < 0.05$ and an extremely significant at $P < 0.01$. The cumulative mortality of the shrimp was analysed by the log-rank test with the Kaplan-Meier method.

3. Results

3.1. Sequence analysis of LvPGK

As a result, a 1855 bp nucleotide sequence representing the full-length cDNA of *LvPGK* was obtained and deposited to GenBank (with accession number of MK734376), which contained an ORF of 1248 bp encoding a polypeptide of 415 amino acids residues (aa), an 84 bp 5' -untranslated region (UTR), a 523 bp 3' -UTR and a poly A tail (Fig. 1). The calculated molecular weight of deduced polypeptide was 44.26 kDa and theoretical isoelectric point (pI) was 6.62. A N-glycosylation site was predicted at position of Asn^{348} (Fig. 1A) and a conserved PGK domain was predicted at positions of 8–404 aa (Fig. 1B).

Multiple alignments showed that the amino acid sequence of *LvPGK* shared the highest identity with the PGK from an amphipod crustacean *Hyalella azteca* (81.5%) and had high identity with the PGK from human (75.1%), zebrafish (72.9%), fruit fly (74.9%) and other organisms (Table 2). The conservative substrate binding sites (5 residues), ADP binding sites (11 residues) and hinge region (7 residues) in PGK family were also identified in *LvPGK* (Fig. 2A). Phylogenetic analysis showed that the predicted PGK amino acids of vertebrates and invertebrates were clustered to their corresponding subgroups. *LvPGK* belonged to the group of invertebrates and had the closest phylogenetic relationship with PGK from the crustacean *H. azteca* (Fig. 2B).

3.2. Expression analysis of LvPGK

The tissue distribution of *LvPGK* transcripts is shown in Fig. 3. *LvPGK* showed a ubiquitous expression in all examined tissues. The most predominant expression of *LvPGK* was detected in the muscle, followed by the heart, stomach and gill tissues, and the expression levels of *LvPGK* in intestine, hemocytes, nerve and hepatopancreas were very weak.

The expression patterns of *LvPGK* in shrimp hemocytes and hepatopancreas after WSSV challenge are shown in Fig. 4. *LvPGK* transcripts upregulated significantly ($P < 0.05$) in hemocytes at 6 h, reaching the greatest expression level at 24 h, which was approximate 6.91-fold greater than that of the control ($P < 0.01$). Then, the expression of *LvPGK* declined gradually from 48 h to 96 h post injection, however it was still significantly higher than that of the control at 96 h ($P < 0.05$) (Fig. 4A). The expression level of *LvPGK* in the hepatopancreas was similar to that in the hemocytes, with the peak value was approximate 5.82-fold higher than that of the control at 24 h ($P < 0.01$). Then, it decreased significantly from 48 h to 96 h, and the lowest value was approximate 14.7% of the control at 96 h ($P < 0.01$).

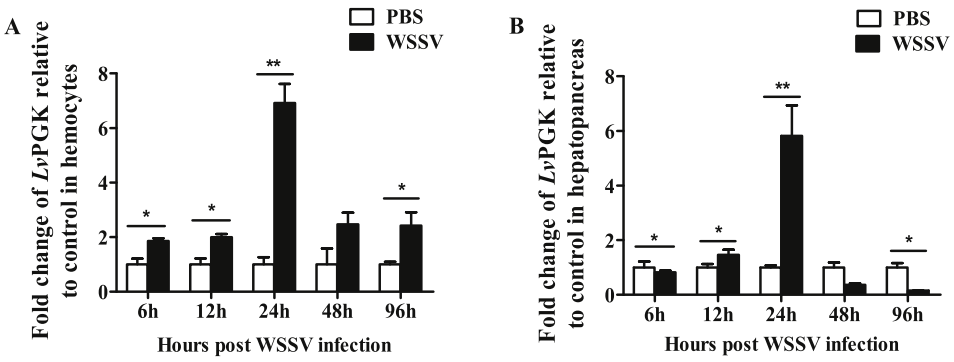

Fig. 4. Expression of *Lv*PGK in hemocytes (A) and hepatopancreas (B) at 6 h, 12 h, 24 h, 48 h and 96 h after WSSV infection in shrimp. The *Lv*PGK expression levels were normalized to that of *Lv*β-actin, and the PBS control at each time point was set as 1. The results were based on three independent cDNA samples and expressed as the mean ± SE (N = 3). Sing asterisk (*) represents significant difference ($P < 0.05$), and double asterisk (**) represents extreme significant difference ($P < 0.01$).

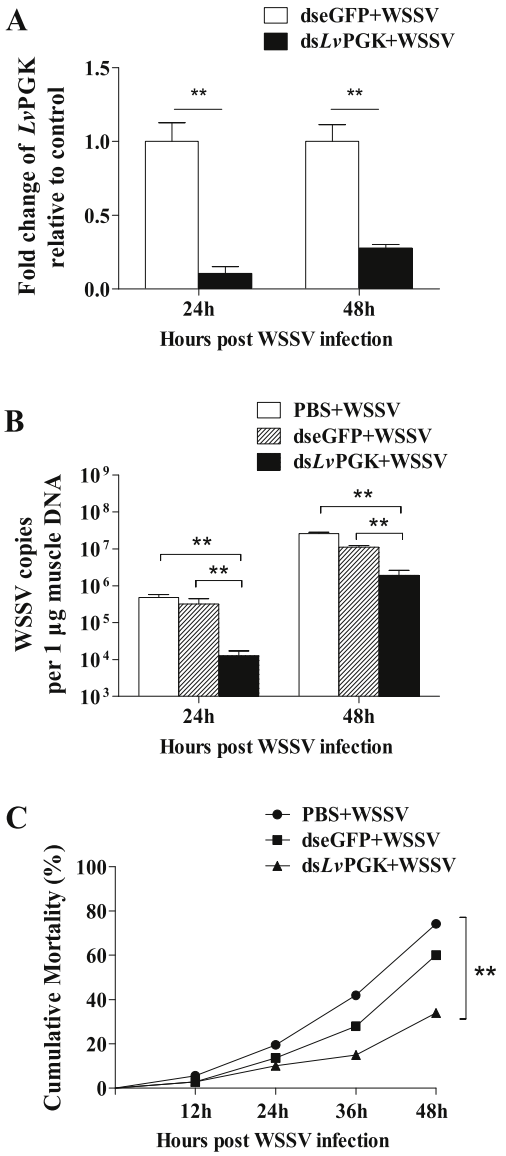

Fig. 5. WSSV copies and cumulative mortality of *Lv*PGK RNAi shrimp after WSSV infection. (A) qPCR analysis of the silencing efficiency of *Lv*PGK, with an internal control of *Lv*β-actin. The results were based on three independent cDNA samples and expressed as the mean ± SE (N = 3). (B) WSSV copies per 1 μg muscle tissue genome DNA were measured at 24 h and 48 h after WSSV infection. Bars indicate the mean ± SE of three independent genomic DNA samples (N = 3). (C) Cumulative mortality of *Lv*PGK silencing shrimp after WSSV infection. The data were analysed using the Kaplan-Meier method, and significant differences were detected by the log-rank test. Sing asterisk (*) represents significant difference ($P < 0.05$), and double asterisk (**) represents extreme significant difference ($P < 0.01$).

3.3. Effects of LvPGK RNAi on the WSSV replication and shrimp cumulative mortality

To further investigate the role of *LvPGK* during WSSV infection, RNAi was used to silence *LvPGK* expression. QPCR showed that injection with 3 μg/g shrimp ds*LvPGK* significantly downregulated the expression of *LvPGK* ($P < 0.01$) (Fig. 5A). Therefore, WSSV challenge was carried out at 24 h after ds*LvPGK* injection.

WSSV copy numbers in *LvPGK* silencing shrimp are shown in Fig. 5B. The WSSV copies in the *LvPGK* silencing group were significantly lower than those of the PBS and eGFP silencing control group, and they reached the values of ~2.7% and ~4.0% of the PBS and dseGFP control at 24 h ($P < 0.01$) and ~7.3% and ~17.2% of the PBS and dseGFP control at 48 h ($P < 0.01$), respectively.

The cumulative mortality of *LvPGK* silencing shrimp after WSSV infection is shown in Fig. 5C. Shrimp mortality increased gradually in all groups after WSSV injection. However, compared with the control, a significantly lower cumulative mortality was found in the *LvPGK* silencing group after 48 h virus challenge ($P < 0.01$) (33.8% cumulative mortality of the *LvPGK* knockdown group, 74.2% cumulative mortality of the PBS control group and 60.0% cumulative mortality of the dseGFP control group).

3.4. WSSV infection-induced changes in the metabolites of LvPGK RNAi shrimp

The changes of some biochemical products in hepatopancreas and muscle of *LvPGK* silencing shrimp after WSSV infection are shown in Fig. 6. Compared with the control group, no significant change of glucose concentration was detected in the hepatopancreas of the *LvPGK* silencing shrimp after WSSV infection (Fig. 6A). However, the pyruvate concentration decreased significantly in the *LvPGK* silencing group, with the lowest value approximating 46.2% of the eGFP silencing control appeared at 0 h after WSSV injection (24 h after *LvPGK* RNAi) ($P < 0.01$). And the significant low concentration maintained to 48 h post-injection ($P < 0.01$) (Fig. 6B). The concentration of lactate in *LvPGK* silencing shrimp also decreased significantly from 0 to 48 h after WSSV injection, with the lowest value of approximating 44.4% as much as that of the control appeared at 0 h ($P < 0.05$) (Fig. 6C).

In muscle tissue, the glucose concentration did not show significant change in the *LvPGK* silencing shrimp from 0 to 48 h after WSSV infection (Fig. 6D). The concentration of pyruvate decreased significantly in the *LvPGK* silencing shrimp from 0 to 48 h after challenge ($P < 0.05$), with the lowest value of approximating 32.1% as much as the control appeared at 48 h (Fig. 6E). The lactate concentration also decreased significantly in *LvPGK* silencing shrimp from 0 to 24 h after WSSV injection, with the lowest value of approximating 56.3% of the control at 0 h ($P < 0.05$), however, it recovered to the control level at 48 h after WSSV injection (Fig. 6F).

3.5. Expression of some antimicrobial peptide genes in LvPGK RNAi shrimp after WSSV challenge

The expression levels of crustin, ALF1, ALF2 and ALF3 in the hepatopancreas of *LvPGK* silencing shrimp infected with WSSV are shown in Fig. 7. The expression of crustin was reduced after *LvPGK* silencing, and after WSSV infection, crustin transcripts dramatically decreased at 24 h and 48 h, reaching the lowest value of ~22.3% as much as the dseGFP appearing control at 24 h ($P < 0.05$) (Fig. 7A). When *LvPGK* was silenced, the expression level of ALF1 significantly declined, reaching the lowest level of ~15.0% of the control ($P < 0.05$). Then it increased gradually and returned to the control level at 48 h after WSSV challenge (Fig. 7B). The transcriptional level of ALF2 and ALF3 decreased after *LvPGK* silencing, with the lowest values of ~34.3% and ~30.4% as much as the control appearing at 48 h after WSSV injection, respectively ($P < 0.05$) (Fig. 7C and D).

4. Discussion

In the present study, *LvPGK* was first cloned and characterized in shrimp. The full-length cDNA sequence of the *LvPGK* gene was 1855 bp, including a 1248 bp ORF encoding a polypeptide of 415 amino acids (Fig. 1A). The typical PGK domain was also predicted in *LvPGK* (Fig. 1B), suggesting that *LvPGK* might belong to the conservative PGK family. The conserved crucial catalytic domains of PGK functioned as binding substrates, ADP and active configuration were predicted in *LvPGK* (Fig. 2A), indicating that PGK is a highly conserved enzyme in species and *LvPGK* might possess the catalytic function of the PGK

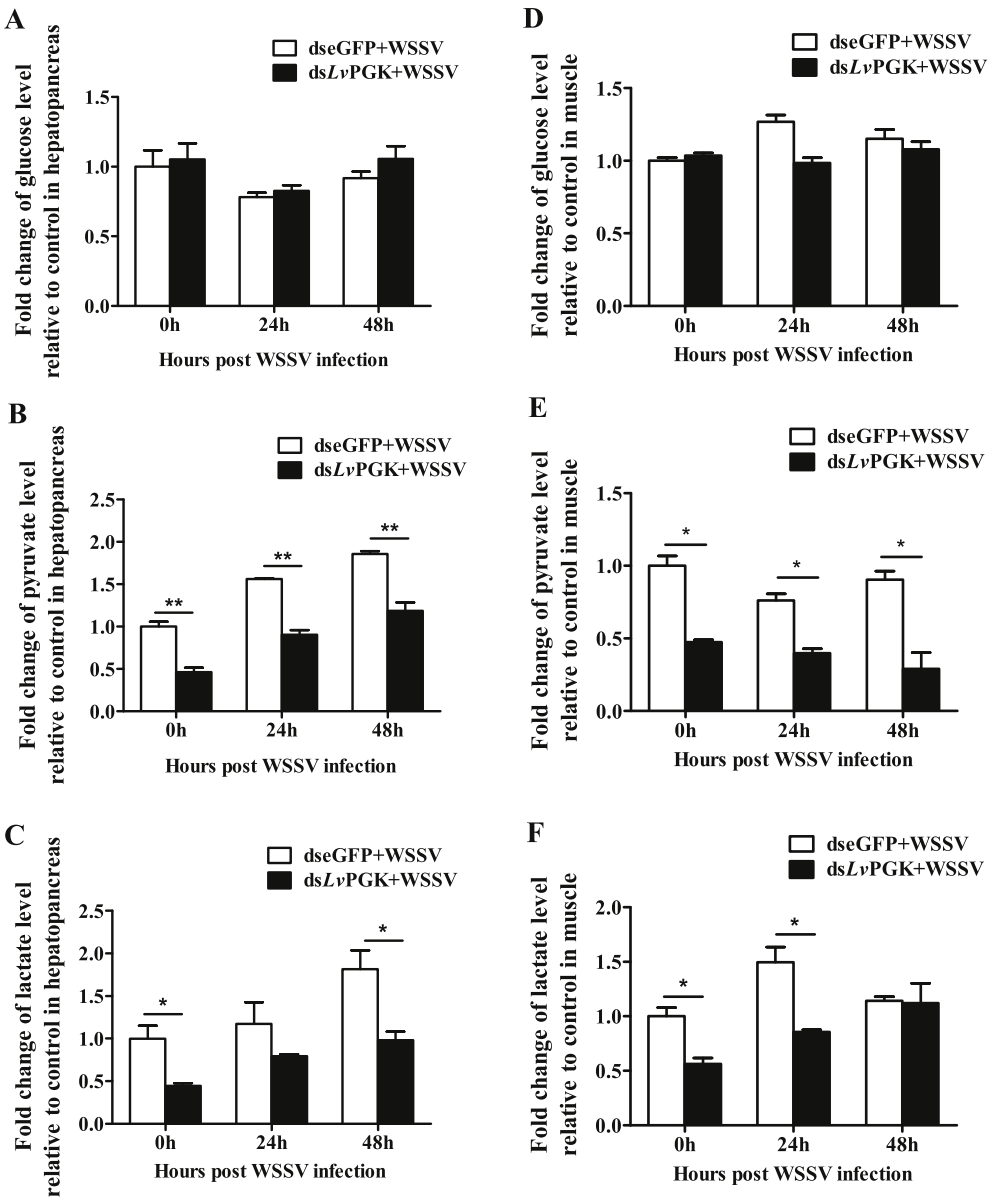

Fig. 6. The concentration of glucose, pyruvate, lactate in hepatopancreas and muscle of *Lv*PGK silencing shrimp after WSSV infection. WSSV injection was carried out at 24 h after *Lv*PGK RNAi, samples were collected from the *Lv*PGK silencing shrimp at 0 h (24 h after *Lv*PGK silencing), 24 h and 48 h after WSSV injection. Glucose level (A), pyruate level (B) and lactate level (C) in the hepatopancreas; and glucose level (D), pyruate level (E) and lactate level (F) in the muscle. The dseGFP control at 0 h was set as 1. Bars indicate the mean ± SE of three parallel samples (N = 3). Sing asterisk (*) represents significant difference ($P < 0.05$), and double asterisk (**) represents extreme significant difference ($P < 0.01$).

family [31]. Multiple sequence alignments and phylogenetic analysis showed that *LvPGK* shared high identities with PGK from other invertebrates and vertebrates, with the closest relationship with PGK from an amphipod crustacean *H. azteca* (Fig. 2B). The observed relationships within this cluster reflected the taxonomic positions of the species.

LvPGK was broadly expressed in most examined tissues, with the highest expression in muscle, followed by heart and brain, and the lowest level was found in intestine (Fig. 3). Our results suggested that muscle and heart might play a more important role in synthesizing PGK in *L. vannamei*, which might be due to high energy metabolism and requirements of these tissues. However, the expression levels of *LvPGK* in the immune tissues including hepatopancreas and hemocytes were very low, suggesting that these immune tissues do not maintain high energy metabolism levels in the normal shrimp [32].

In invertebrates, the hepatopancreas and hemocytes are important tissues involved in the immune response. The significant upregulations of *LvPGK* transcripts were detected in both tissues after WSSV infection (Fig. 4), indicating that *LvPGK* might be induced in the anti-WSSV immune response of shrimp. However, a previous study showed that no significant change of PGK protein content was detected in the hemocytes of *L. vannamei* after WSSV infection [4], which was different from our results. The difference might be due to different physiological status of the shrimp or the PGK was detected based on the different expression levels.

Energy metabolism plays an important role in shrimp immune response. Our results showed that the WSSV copy numbers decreased significantly in *LvPGK* RNAi shrimp (Fig. 5B), suggesting that *LvPGK* silencing might affect the energy production in the glycolysis, which would result to failure meeting the increasing requirements of viral replication. WSSV is a large enveloped virus, and it was demonstrated that a large amount of phospholipids might be required to form a viral envelope during the viral replication and package [33,34]. A similar result was observed in shrimp *Exopalaemon carinicauda* with WSSV infection, which showed that triosephosphate isomerase (TPI) gene silencing led to decrease of downstream metabolic products and then resulted in the decrease of phospholipid synthesis and eventually a lower virus replication in infected shrimp [35]. In addition, the enzyme PGK catalyses 1,3-diphosphoglycerate to 3-phosphoglycerate, which is used to further synthesize phospholipid [4]. Our results indicated that *LvPGK* silencing might lead to the disorder of glycolysis, and then resulted to the decrease of downstream molecules production,

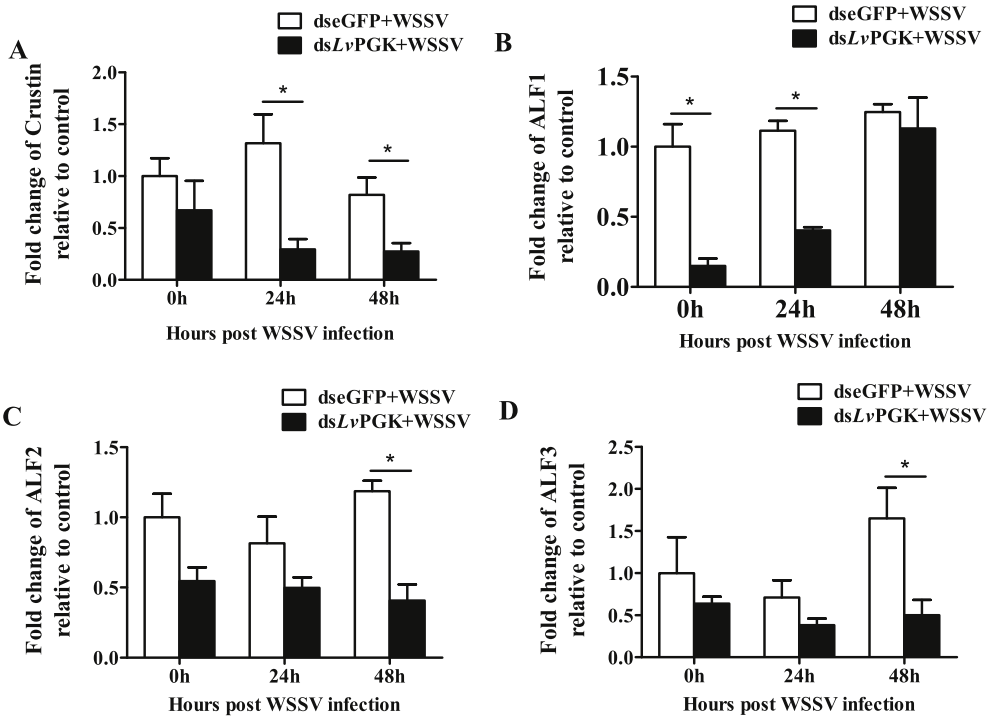

Fig. 7. The changes of immune-related genes in *Lv*PGK silencing shrimp after WSSV infection. The expression levels of crustin (A), ALF1 (B), ALF2 (C) and ALF3 (D) were normalized to *Lv*β-actin. The dseGFP control at 0 h was set as 1. The results were based on three parallel cDNA samples and expressed as the mean ± SE (N = 3). Sing asterisk (*) represents significant difference ($P < 0.05$), and double asterisk (**) represents extreme significant difference ($P < 0.01$).

phospholipid synthesis, and the decline of WSSV replication (Fig. 5B). Therefore, the cumulative mortality of shrimp decreased (Fig. 5C). Similarly, another investigation demonstrated that WSSV replication was significantly reduced after the expression of Ras GTPase suppressed [36], which agreed with our results.

In addition, glucose is one of the most important energy resources. Glucose consumption and lactate accumulation were observed in *L. vannamei* during the WSSV replication [37]. The increasing of glucose, lactate, and other biochemical products were also observed in the hepatopancreas after shrimp infected with IHHNV [19] and WSSV [38]. These transformations indicated that viral infection might cause temporary changes in host metabolic pathways to maximize proliferation. Our results showed that no significant change of glucose content was detected in the hepatopancreas and muscle tissue of *LvPGK* RNAi shrimp after WSSV infection (Fig. 6A–D), which might be due to the involvement and compensation from other metabolic pathways. Furthermore, pyruvate and lactate levels decreased significantly (Fig. 6B, C, 6E, 6F), which might be due to the decrease of metabolic products caused by *LvPGK* silencing and the increase of energy requirements of WSSV replication and immune response. However, the mechanisms need to be further studied.

Antimicrobial peptides (AMPs) are generally considered as essential immune effectors in innate immune response through killing a wide range of pathogens. Previous research has showed that crustin and ALFs played a crucial role in shrimp anti-WSSV infection immune response [39–41]. Our findings showed that the downregulation of crustin, ALF1, ALF2 and ALF3 expression in *LvPGK* silencing shrimp and after WSSV challenge (Fig. 7), suggesting that the expression of these AMPs could not be induced in shrimp after *LvPGK* silencing, which might be due to the metabolic disorder and the decrease energy production after *LvPGK* silencing. It was demonstrated that knockdown a crucial enzyme in lipogenic and glycogenic, myocyte enhancer factor-2 (MEF2), resulted to reduced expression of AMPs [42]. The decline of both WSSV replication and these AMP genes were detected in our study, suggesting that knockdown of *LvPGK* might lead to suppression of WSSV replication due to metabolic change. Then less WSSV numbers might not induce a rapid immune response. Additionally, there are many other immune genes were involved in shrimp immune response, which might contribute to the decrease of WSSV replication and shrimp mortality. Therefore, the expression levels of more immune genes need to be further investigated.

In conclusion, the full-length cDNA sequence of *LvPGK* was cloned in shrimp *L. vannamei*. *LvPGK* was broadly expressed in most examined tissues with the highest level in the muscle and the lowest level in the intestine. The expression of *LvPGK* in hepatopancreas and hemocytes could be induced by WSSV infection. Interestingly, WSSV replication and shrimp mortality decreased significantly after *LvPGK* silencing. Moreover, the changing of metabolic products might affect WSSV replication and some immune genes' expression and induction.

[10].

Acknowledgements

This research was supported by Science and Technology Program of Jimei (20172C01) and NSFC 41276178.

References

[1] G.D. Stentiford, K. Sritunyalucksana, T.W. Flegel, B.A.P. Williams, B. Withyachumnarnkul, O. Itsathitphaisarn, et al., New paradigms to help solve the global aquaculture disease crisis, PLoS Pathog. 13 (2017) e1006160.
[2] T.W. Flegel, Historic emergence, impact and current status of shrimp pathogens in Asia, J. Invertebr. Pathol. 110 (2012) 166–173.
[3] S. Thitamadee, A. Prachumwat, J. Srisala, P. Jaroenlak, P.V. Salachan, K. Sritunyalucksana, et al., Review of current disease threats for cultivated penaeid shrimp in Asia, Aquaculture 452 (2016) 69–87.
[4] M.A. Su, Y.T. Huang, I.T. Chen, D.Y. Lee, Y.C. Hsieh, C.Y. Li, et al., An invertebrate Warburg effect: a shrimp virus achieves successful replication by altering the host metabolome via the PI3K-Akt-mTOR pathway, PLoS Pathog. 10 (2014) e1004196.
[5] C.Z. Li, S.P. Weng, J.G. He, WSSV–host interaction: host response and immune evasion, Fish Shellfish Immunol. 84 (2019) 558–571.
[6] C.S. Cheng, H.C. Wang, Lipid metabolism during WSSV infection in shrimp, Fish Shellfish Immunol. 53 (2016) 59.
[7] F.F. Ma, Q.H. Liu, G.K. Guan, C. Li, J. Huang, Arginine kinase of *Litopenaeus vannamei* involved in white spot syndrome virus infection, Gene 539 (2014) 99–106.
[8] L. Yang, J. Liu, M. Liu, M. Qian, M.Z. Zhang, H.J. Hu, Identification of fatty acid synthase from the Pacific white shrimp, *Litopenaeus vannamei* and its specific expression profiles during white spot syndrome virus infection, Fish Shellfish Immunol. 30 (2011) 744–749.
[9] X.P. Li, X.H. Meng, K. Luo, S. Luan, B.X. Cao, J. Kong, cDNA cloning and expression analysis of a phosphopyruvate hydratase gene from the Chinese shrimp *Fenneropenaeus chinensis*, Fish Shellfish Immunol. 63 (2017) 173–180.

[10] R.D. Banks, C.C.F. Blake, P.R. Evans, R. Haser, D.W. Rice, G.W. Hardy, et al., Sequence, structure and activity of phosphoglycerate kinase: a possible hinge-bending enzyme, Nature 279 (1979) 773–777.
[11] A. Yoshida, Hematologically important mutations: molecular abnormalities of phosphoglycerate kinase, Blood Cells Mol. Dis. 22 (1996) 265–267.
[12] A.J. Lay, X.M. Jiang, O. Kisker, E. Flynn, A. Underwood, R. Condron, et al., Phosphoglycerate kinase acts in tumour angiogenesis as a disulphide reductase, Nature 408 (2000) 869–873.
[13] Z.F. Duan, D.E. Lamendola, R.Z. Yusuf, R.T. Penson, F.I. Preffer, M.V. Seiden, Overexpression of human phosphoglycerate kinase 1 (PGK1) induces a multidrug resistance phenotype, Anticancer Res. 22 (2002) 1933–1941.
[14] J.H. Wang, J.C. Wang, J.L. Dai, Y.H. Jung, C.L. Wei, Y. Wang, et al., A glycolytic mechanism regulating an angiogenic switch in prostate cancer, Cancer Res. 67 (2007) 149–159.
[15] T. Ogino, M. Iwama, J. Kinouchi, Y. Shibagaki, T. Tsukamoto, K. Mizumoto, Involvement of a cellular glycolytic enzyme, phosphoglycerate kinase, in Sendai virus transcription, J. Biol. Chem. 274 (1999) 35999–36008.
[16] S.J. Hong, K.Y. Seong, W.M. Sohn, K.Y. Song, Molecular cloning and immunological characterization of phosphoglycerate kinase from *Clonorchis sinensis*, Mol. Biochem. Parasitol. 108 (2000) 207–216.
[17] R. Kumar, P.K. Doharey, J.K. Saxena, S. Rathaur, Molecular cloning, purification and characterization of *Brugia malayi* phosphoglycerate kinase, Protein Expr. Purif. 132 (2017) 152–163.
[18] A. Goel, M.M. Domach, W. Hanley, J.W. Lee, M.M. Ataai, Coordination of glycolysis and TCA cycle reaction networks, Ann. NY. Acad. Sci. 782 (1996) 1–16.
[19] D. Galvanalvarez, F. Mendozacano, J. Hernandezlopez, A. Sanchezpaz, Experimental evidence of metabolic disturbance in the white shrimp *Penaeus vannamei* induced by the Infectious Hypodermal and Hematopoietic Necrosis Virus (IHHNV), J. Invertebr. Pathol. 111 (2012) 60–67.
[20] F. Vargasalbores, G. Yepizplascencia, F. Jimenezvega, A. Avilavilla, Structural and functional differences of *Litopenaeus vannamei* crustins, Comp. Biochem. Physiol. B 138 (2004) 415–422.
[21] E.D.L. Vega, N.A. O'Leary, J.E. Shockey, J. Robalino, C. Payne, C.L. Browdy, et al., Anti-lipopolysaccharide factor in *Litopenaeus vannamei* (LvALF): a broad spectrum antimicrobial peptide essential for shrimp immunity against bacterial and fungal infection, Mol. Immunol. 45 (2008) 1916–1925.
[22] M. Li, C.X. Ma, H.Y. Li, J.X. Peng, D. Zeng, X.H. Chen, et al., Molecular cloning, expression, promoter analysis and functional characterization of a new Crustin from *Litopenaeus vannamei*, Fish Shellfish Immunol. 73 (2018) 42–49.
[23] J.W. Liu, Y. Yu, F.H. Li, X.J. Zhang, J.H. Xiang, A new anti-lipopolysaccharide factor (ALF) gene with its SNP polymorphisms related to WSSV-resistance of *Litopenaeus vannamei*, Fish Shellfish Immunol. 39 (2014) 24–33.
[24] X.J. Lv, S.H. Li, F. Liu, F.H. Li, J.H. Xiang, Identification and function analysis of an anti-lipopolysaccharide factor from the ridgetail prawn *Exopalaemon carinicauda*, Dev. Comp. Immunol. 70 (2017) 128–134.
[25] W.Y. Hu, C.L. Yao, Molecular and immune response characterizations of a novel AIF and cytochrome c in *Litopenaeus vannamei* defending against WSSV infection, Fish Shellfish Immunol. 56 (2016) 84–95.
[26] C.L. Yao, P.F. Ji, Z.Y. Wang, F.H. Li, J.H. Xiang, Molecular cloning and expression of NOS in shrimp, *Litopenaeus vannamei*, Fish Shellfish Immunol. 28 (2010) 453–460.
[27] K.J. Livak, T.D. Schmittgen, Analysis of relative gene expression data using real-time quantitative PCR and the $2^{-\Delta\Delta}$CT method, Methods 25 (2001) 402–408.
[28] S. Wang, X. Song, Z.J. Zhang, H.Y. Li, K. Lv, B. Yin, et al., Shrimp with knockdown of LvSOCS2, a negative feedback loop regulator of JAK/STAT pathway in *Litopenaeus vannamei* , exhibit enhanced resistance against WSSV, Dev. Comp. Immunol. 65 (2016) 289–298.
[29] W. Qiu, S. Zhang, Y.G. Chen, P.H. Wang, X.P. Xu, C.Z. Li, et al., *Litopenaeus vannamei* NF-κB is required for WSSV replication, Dev. Comp. Immunol. 45 (2014) 156–162.
[30] P.K. Smith, R.I. Krohn, G.T. Hermanson, A.K. Mallia, F.H. Gartner, M.D. Provenzano, et al., Measurement of protein using bicinchoninic acid, Anal. Biochem. 150 (1985) 76–85.
[31] Y. Hong, L.N. Huang, J.M. Yang, X.D. Cao, Q. Han, M. Zhang, et al., Cloning, expression and enzymatic characterization of 3-phosphoglycerate kinase from *Schistosoma japonicum*, Exp. Parasitol. 159 (2015) 37–45.
[32] T. Dolezal, G. Krejcova, A. Bajgar, Molecular regulations of metabolism during immune response in insects, Insect Biochem. Mol. 109 (2019) 31–42.
[33] C.M. Escobedbonilla, M. Wille, P. Sorgeloos, M. Pensaert, H. Nauwynck, A review on the morphology, molecular characterization, morphogenesis and pathogenesis of white spot syndrome virus, J. Fish Dis. 31 (2010) 1–18.
[34] Y.C. Hsieh, Y.M. Chen, C.Y. Li, Y.H. Chang, S.Y. Liang, S.Y. Lin, et al., To complete its replication cycle, a shrimp virus changes the population of long chain fatty acids during infection via the PI3K-Akt-mTOR-HIF1α pathway, Dev. Comp. Immunol. 53 (2015) 85–95.
[35] F. Liu, S.H. Li, G.X. Liu, F.H. Li, Triosephosphate isomerase (TPI) facilitates the replication of WSSV in *Exopalaemon carinicauda*, Dev. Comp. Immunol. 71 (2017) 28–36.
[36] Y.T. Tsenga, R. Kumara, H.C. Wang, LvRas and LvRap are both important for WSSV replication in *Litopenaeus vannamei*, Fish Shellfish Immunol. 88 (2019) 150–160.
[37] I.T. Chen, T. Aoki, Y.T. Huang, I. Hirono, T.C. Chen, J.Y. Huang, et al., White spot syndrome virus induces metabolic changes resembling the warburg effect in shrimp hemocytes in the early stage of infection, J. Virol. 85 (2011) 12919–12928.
[38] W.W. Fan, Y.F. Ye, Z. Chen, Y. Shao, X.L. Xie, W.W. Zhang, et al., Metabolic product response profiles of *Cherax quadricarinatus* towards white spot syndrome virus infection, Dev. Comp. Immunol. 61 (2016) 236–241.
[39] H.S. Jiang, W.M. Jia, X.F. Zhao, J.X. Wang, Four crustins involved in antibacterial responses in *Marsupenaeus japonicus*, Fish Shellfish Immunol. 43 (2015) 387–395.
[40] T. Methatham, P. Boonchuen, P. Jaree, A. Tassanakajon, K. Somboonwiwat, Antiviral action of the antimicrobial peptide ALF Pm 3 from *Penaeus monodon* against white spot syndrome virus, Dev. Comp. Immunol. 69 (2016) 23–32.
[41] S.H. Li, S.Y. Guo, F.H. Li, J.H. Xiang, Characterization and function analysis of an anti-lipopolysaccharide factor (ALF) from the Chinese shrimp *Fenneropenaeus chinensis*, Dev. Comp. Immunol. 46 (2014) 349–355.
[42] R.I. Clark, S.W.S. Tan, C.B. Péan, et al., MEF2 is an in vivo immune-metabolic switch, Cell 155 (2013) 435–447.